



# **Gradients of cyclic indentation mechanical properties in PR520 epoxy and its 3D carbon fiber composite induced by aging at 150 °C**

M. Pecora, O. Smerdova, M. Gigliotti

## **► To cite this version:**

M. Pecora, O. Smerdova, M. Gigliotti. Gradients of cyclic indentation mechanical properties in PR520 epoxy and its 3D carbon fiber composite induced by aging at 150 °C. *Polymer Degradation and Stability*, 2021, 193, pp.109720. <10.1016/j.polymdegradstab.2021.109720>. <hal-03681132>

**HAL Id: hal-03681132**

**<https://hal.science/hal-03681132v1>**

Submitted on 16 Oct 2023

**HAL** is a multi-disciplinary open access archive for the deposit and dissemination of scientific research documents, whether they are published or not. The documents may come from teaching and research institutions in France or abroad, or from public or private research centers.

L'archive ouverte pluridisciplinaire **HAL**, est destinée au dépôt et à la diffusion de documents scientifiques de niveau recherche, publiés ou non, émanant des établissements d'enseignement et de recherche français ou étrangers, des laboratoires publics ou privés.



Distributed under a Creative Commons CC BY-NC 4.0 - Attribution - Non-commercial use - International License

# Gradients of cyclic indentation mechanical properties in PR520 epoxy and its 3D carbon fibre composite induced by aging at 150°C

M. Pecora<sup>\*</sup> <sup>present address b,</sup> O. Smerdova <sup>a,</sup> M. Gigliotti <sup>a</sup>

a. Institut Pprime, CNRS, ISAE-ENSMA (Department of Physics and Mechanics of Materials),  
Université de Poitiers, 1, Avenue Clément Ader, F-86962 Futuroscope Chasseneuil, France

b. Université de Strasbourg, CNRS, INSA Strasbourg, Institut Charles Sadron, F-67000  
Strasbourg, France

<sup>\*</sup>Corresponding author: [mpecora@unistra.fr](mailto:mpecora@unistra.fr), +33 (0) 388 414 011, Institut Charles Sadron  
UPR22, 23, Rue du Loess, F-67000 Strasbourg, France

**Abstract.** A cyclic indentation test was carried out on PR520 epoxy resin and its 3D interlock carbon fiber reinforced composite in order to study the effects of thermo-oxidative ageing on the material local properties. Thermal ageing has been performed in air at 150°C, which is close to the service temperature in warm zones of aircrafts, for different durations. Two parameters have been considered in this study: the reload indentation modulus, representative of the elastic response, and the ratio between irreversible and total indentation energy, representative of plastic (first cycle) and viscoelastic response. The analysis of cyclic indentation curves shows that elastic and plastic behaviour are affected by thermal ageing, while viscoelastic behaviour is not. Moreover, a gradient of local properties has been measured through the thickness of aged samples. The affected zone extends of about 150µm from the surface exposed to the oxidative environment, while the properties of the sample core are similar to those of the virgin material. Property gradient profiles measured on resin and composite aged in the same conditions are well superposed.

Key-words: Epoxy resin, carbon fiber composites, instrumented indentation, thermal-ageing

## 1. Introduction

The growing use of polymer-matrix composites in the “warm zones” of aircraft structures leads to the necessity to understand the degradation phenomena due to their exposure at elevated temperatures. In these “warm” zones, the temperature range is between 150 and 300°C that, together with the presence of oxygen, create environmental conditions conducive to degradation phenomena of the polymer matrix over long time of exposure. For temperatures lower than glass transition temperature, the polymer degradation is most often due to pure thermal oxidation, while for temperatures higher than the glass transition, secondary anaerobic degradation phenomena (thermolysis) could also occur. In the specific case of thermo-oxidative aging, an evolution of local mechanical properties occurs due to the change in macromolecular structure caused by the interaction with oxygen promoted by high temperatures [1]. The visual effect of thermal oxidation of polymers is the change of surface colour [2-9]. In particular, the thermally aged sample appears darker than the virgin one and this change is more significant as the aging conditions are severer. This darker layer, which corresponds to the oxidised zone as opposed to the non-oxidised polymer core, has a thickness of several hundreds of micrometres at most [9]. Because of this small size of the affected zone, instrumented indentation turns out to be the most suitable experimental technique to measure possible gradients of mechanical property in the oxidised layer. In its classical form, instrumented indentation consists in driving a small hard tip of several microns, usually made of diamond, which shape is known at nanometric scale, into the surface of the material under either load or displacement control. The force and displacement data are recorded during the test and analysed to

obtain mechanical properties of the tested material. The most often, indentation protocol is composed by loading and unloading, sometimes completed with a dwell at the maximum load. The application of the Oliver and Pharr analysis method [10] allows to determine two mechanical properties of the material: the Elastic Indentation Modulus  $E^*$  and the Hardness  $H$ .

The instrumented indentation test has been used in numerous previous studies [3-8] to trace the evolution of elastic indentation modulus from the external surface to the core of thermally aged polymer samples, highlighting the presence of a gradient through the sample thickness. In most of the cases, an increase of indentation modulus is observed near the surface directly exposed to the oxidative environment, where it reaches its maximum value. Then, the indentation modulus decreases in the oxidized layer and reaches a value close to that of the virgin material at the sample core. Even if the Oliver and Pharr analysis method is widely used in the literature to derive elastic indentation modulus and hardness of polymers, many studies have highlighted the difficulties that arise from its application on load-displacement curves resulting from indentation of polymeric surfaces [11-16]. In fact, the hypothesis of elastic unloading, on which the Oliver and Pharr analysis method is based, turns out to be too strong on unloading curves of polymers, in which creep phenomena occurs because of their viscoelastic nature. Moreover, time independent properties like elastic modulus and hardness are not sufficient to fully describe the complex time dependent behaviour of polymers. Therefore, in this work, a cyclic indentation testing method developed previously for polymers (see [17]) has been used to characterize the environmental effects, not only on elastic, but also on plastic and viscoelastic local behaviour.

The aim of this study is to characterise the gradients of mechanical properties of PR520 epoxy resin used in aeronautical application due to thermal aging at 150°C, which is higher than in the previous studies and closer to the glass transition of this polymer. Moreover, the effect of thermal aging on the local time dependent properties of the same material as a matrix of a 3D interlock carbon fiber reinforced composite aged in the same conditions has been studied as well. This paper is organised as follows. After the presentation of the materials and the cyclic indentation method, the results are grouped into three parts. Firstly, the indentation loops of the virgin resin and its composite and their shift by material aging are presented and discussed. Secondly, the mechanical properties from the tests on the exposed surface are obtained and presented. Finally, the gradients of cyclic mechanical properties in the thickness of polymer and composite samples are plotted and discussed.

## **2. Materials and methods**

### **2.1. Materials**

The material used in this study is the PR520 epoxy resin, a thermoset polymer used as matrix of carbon fiber reinforced composites, commonly employed in the aerospace industry. Neat epoxy resin was provided by Cytac Engineered Materials in the form of 1 cm thick plates, from which several samples with a thickness of 3.5 mm were cut transversally.

The composite material is a 3D interlock reinforced with carbon fibers and manufactured through Resin Transfer Molding process. It was provided by SAFRAN in the form of 3 cm thick plates. This kind of composite architecture provides a high number of large resin

pockets in which the polymer matrix can be locally tested by instrumented indentation avoiding any constraint effect induced by the more rigid carbon fiber bundles [19-21]. To make the surface state suitable for instrumented indentation measurements, the polymer and composite samples have been mechanically polished by grinding and finishing. Both epoxy resin and composite samples were conditioned in air at 150°C, a temperature value close to that found in "warm zones" of aircraft structures, for 220h, 520h and 1005h. Although severe, these conditions did not induce any visible oxidation-induced damage. Differential Scanning Calorimetry has been performed on virgin and aged samples in order to measure glass transition temperature. The DSC testing protocol employed consists in two heating cycles from 30°C to 280°C. The heating rate was set at 2°C/min while the cooling rate at 5°C/min. As it can be observed from the reversible heat flow vs temperature plot, Figure 1, the  $T_g$  value measured on the virgin resin (continuous line) is  $159\pm1^\circ\text{C}$ . Moreover, a slight decrease in  $T_g$  has been measured on the oxidised layer of the aged resin samples, as it can be observed in Figure 1 where the DSC thermogram for the higher ageing time is also reported (dashed line). The ageing temperature employed in this study is slightly lower than the PR520 epoxy resin glass transition temperature, but the thermogram shows that the transition started before this temperature.

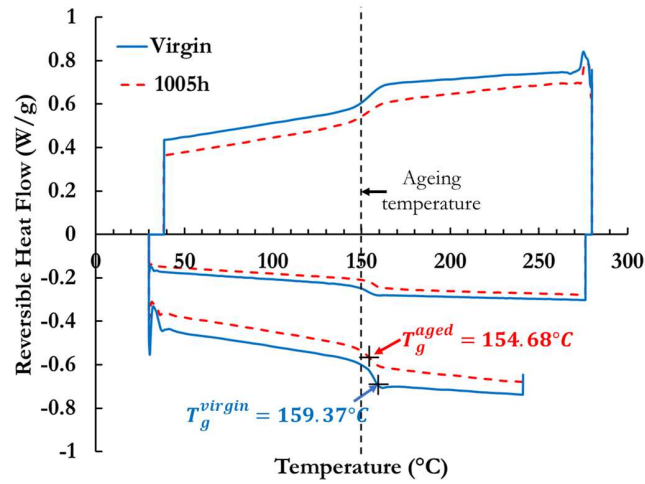


Figure 1. Reversible Heat Flow vs Temperature plot obtained by DSC on virgin (continuous blue line) and aged for 1005h (dashed red line) PR520 epoxy resin.

In order to evaluate the change of mechanical properties due to thermal aging, instrumented indentation tests have been carried out on the external surface and on the cross section, at different distances from the exposed surface, of the conditioned resin and composite samples. Two samples for each aging condition were thus needed: one to be tested on the surface that has been preliminary polished (before aging) and the other to be tested through the thickness that has been prepared following the scheme reported in Figure 2.

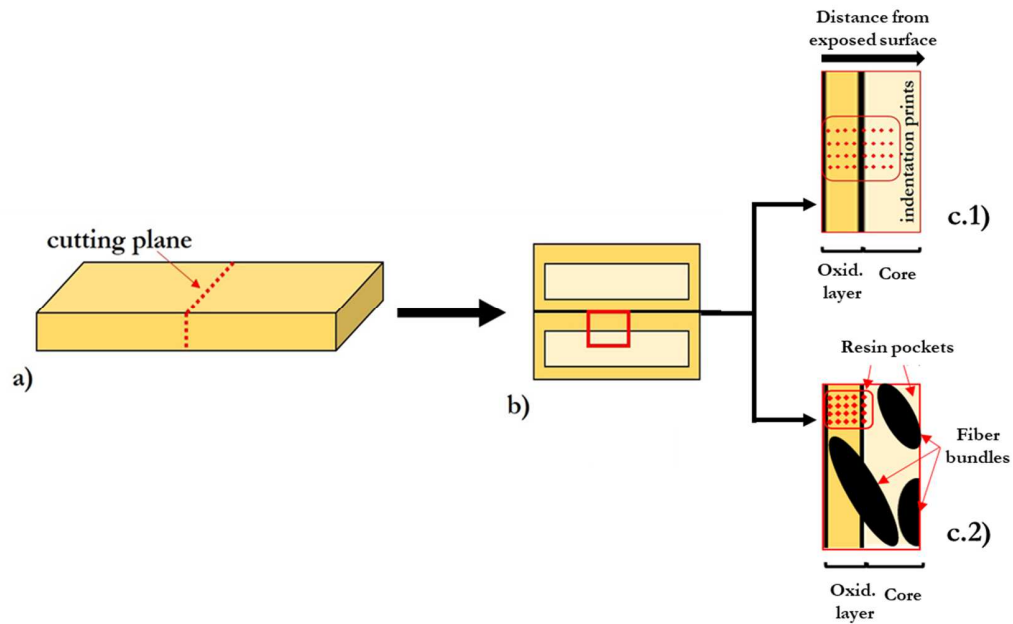


Figure 2. Sample preparation for instrumented indentation tests through the thickness of aged epoxy resin (c.1) and composite (c.2) samples

Figure 2 highlights that the aged samples were cut perpendicularly to the exposed surface (a), then, the two sides were embedded together with a clear epoxy (b) and polished. Finally, indentation tests were carried out at different distances from the exposed surface, following a straight path, in order to capture gradient of properties in the oxidized layer (c). In order to avoid the influence of a previous residual print on indentation results, the indentations along the path have been spaced at more than three times the diameter of the residual impression, as suggested by the indentation test standard ISO 14577-2. According to the scheme proposed on the right side of Figure 2 (c.2), the tests on composite samples were performed in the rich matrix zones among fiber bundles, in order to compare the local mechanical properties change due to thermal ageing of the neat resin and the matrix in the composite.



## 2.3 Experimental method

### 2.3.1 Equipment

The instrumented indentation machine used in this study is the Ultra-micro Indenter Fischerscope H100C equipped with a base square pyramid diamond tip Vickers which operates between micro and nano test range. This equipment allows to perform force-controlled tests in a range between 0.1 and 1000  $mN$  with an uncertainty of  $\pm 0.02 mN$ . The maximal measurable depth is 700  $\mu m$  and the uncertainty on the displacement values is  $\pm 2 nm$ . During the tests, load and displacement data are recorded every 0.1 s.

### 2.3.2 Cyclic indentation test

An instrumented indentation cyclic test (Figure 3a) is proposed here to study time-dependent behaviour of polymer materials at the microscopic scale. Further details of this particular indentation method could be find in a previous work [17].

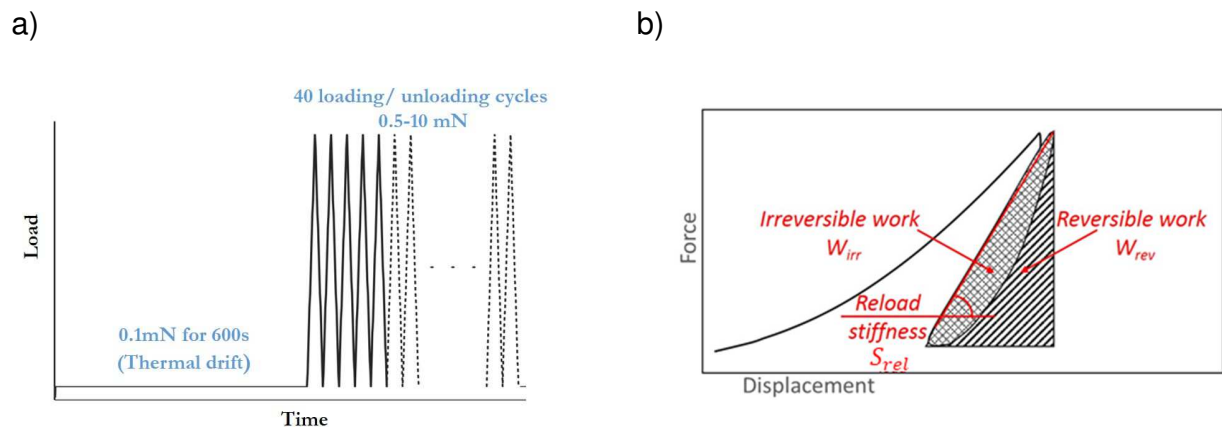


Figure 3. Cyclic instrumented indentation tests loading path (a) and parameters extracted from cyclic force-displacement indentation curves (b).

The initial load hold phase, introduced to evaluate thermal drift, is followed by 40 load-unload cycles between 0.5 and 10 *mN* at constant loading and unloading rate of 2 *mN/s*. This number of cycles was chosen as a compromise between the duration of test and the potential stabilisation of the viscoelastic behaviour. The minimal load is kept positive to constantly maintain contact with the indenter in order to avoid error accumulation due to thermal drift and zero position determination. This study of the effect of thermal ageing on PR520 epoxy resin and composite will rely on two main parameters:

- The instantaneous elastic modulus at each cycle, or reload modulus ( $E_{rel}^*$ ), calculated as:

$$E_{rel}^* = \frac{1}{\frac{1}{E_{r\_rel}} - \frac{1-\nu_i^2}{E_i}} \quad (1)$$

where  $E_i$  and  $\nu_i$  are the elastic modulus and the Poisson's ratio of the indenter, while  $E_{r\_rel}$  is the reduced modulus of the tested material, calculated as:

$$E_{r\_rel} = \frac{\sqrt{\pi}}{2\beta\sqrt{A_p}} S_{rel} \quad (2)$$

In the Eq. 2,  $A_p$  is the projected contact area calculated from the measured contact depth through the calibrated indenter area function,  $\beta$  is a shape factor equal to 1.012 for Vickers indenter and  $S_{rel}$  is the stiffness representing the slope of the reload curves at the peak load (Figure 3b).

It is common to evaluate the indentation elastic modulus from the stiffness at the unload according to the Oliver and Pharr method [10]. However, our previous work revealed that the unloading curve was less suited for viscoelastic materials due to its inconsistency with the Sneddon's elastic solution of the contact between a cone and a flat surface [18]. The reloading curves, on the contrary, are

close to linear, which relates almost constant contact area during the loading. The discussion of the advantages of unloading versus reloading moduli can be found in [17]. In the present study, the reload modulus will be used to describe the evolution of local elastic behaviour with cycles and with the progress of thermal ageing. The unloading elastic modulus is presented in the Supplementary Material to facilitate the comparison of these results to other studies.

- The dissipated energy normalized by the indentation work, or energy ratio ( $\eta$ ), calculated as:

$$\eta = \frac{W_{irr}}{W_{tot}} \quad (3)$$

where  $W_{irr}$  is the irreversible part of indentation work, represented by the loop area between loading and unloading curves, and  $W_{tot}$  is the total work of indentation, represented by the area under the loading curves (Figure 3b). Both areas are calculated through a trapezoidal numerical integration.

For a purely elasto-plastic behaviour relevant to the Oliver and Pharr method, no energy dissipation is expected from the second cycle. For a polymer, with an assumption of viscoelastic-plastic behaviour, a change of dissipative regime was observed between the first cycle, attributed to both viscoelastic and plastic dissipation, and other cycles in which only purely viscoelastic dissipation occurred [17]. The area of hysteresis loops in multicycling indentation to increasing load has been used in a previous study as a tracker of viscoelastic property change due to UV irradiation on different polymers [22].

### **3. Results and discussion**

#### **3.1 Indentation loops of virgin and aged resin and composite**

In this Section, the cyclic indentation curves will be presented and discussed. Firstly, the cyclic load-displacement response obtained on virgin PR520 is presented in Figure 4. The first cycle is very large since it encloses plastic and viscoelastic dissipation followed by a significant hysteresis decrease in second cycle and a progressive thinning of the loops. This behaviour indicates that the viscoelastic dissipation tends to vanish with time during the test. Moreover, this curve shows that while the maximum displacement after each cycle increases very slightly, the minimum, or residual, displacement grows significantly faster. This can be attributed to a poor creep behaviour usual for epoxy resins [15] at room temperature, and a fast recovery of a viscoelastic part of residual displacement after the first loading. Therefore, both hysteresis and maximum and minimum displacement evolutions indicate viscoelastic-plastic behaviour of the PR520 epoxy, with a permanent plastic strain installed during the first cycle and a viscoelastic behaviour progressively fading during the test. Since the maximum displacement remains almost constant with cycles, the projected contact area at this point is constant as well and there is no reason to suspect an addition of plasticity during the cycling.

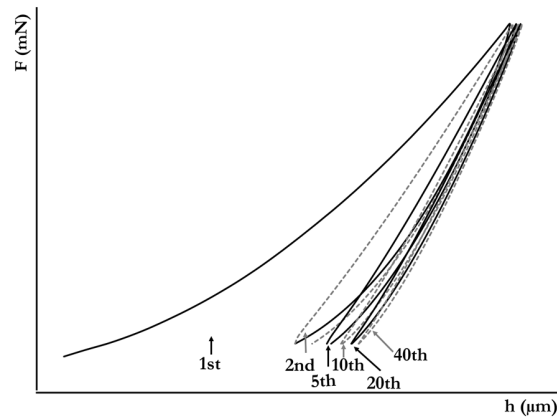


Figure 4. Several indentation loops of virgin epoxy resin

The load-displacement curves averaged of 6 tests for the three aging times and the virgin sample are presented in Figure 5. The indentation curves obtained in the resin pockets located on the surface of the composite samples (dashed lines) are represented as well. For better readability of the graph only measurements performed on the virgin and aged for 1005h composite are reported.

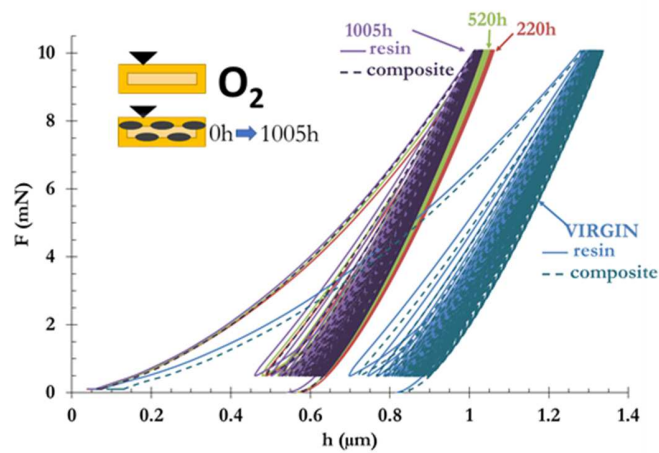


Figure 5. Load displacement curves on the external surface of virgin and thermally aged PR520 epoxy resin and composite samples.

This figure demonstrates that the cyclic indentation behaviour of aged epoxy resin is qualitatively similar to the virgin one, and that is for both neat resin and composite. The loops are also present in aged material and the maximum and minimum displacements progress similarly. However, the load displacement curves are shifted to lower displacement values with ageing time. This observation is similar to that shown by other authors from a simple one cycle indentation of aged resins [3-8]. It can also be seen that the gap between virgin and 220h aged material is much higher than the one between further aging times. This suggests that the oxidation of the external layer of the surface occurs faster than the minimum aging time employed in this study.

Figure 6 depicts the cyclic load-displacement curves (average of 6 tests) obtained at different distances from the exposed surface (from 0 to 240 $\mu\text{m}$ ) of the neat epoxy resin sample aged for 1005h. The curve obtained on the virgin sample surface is reported as well.

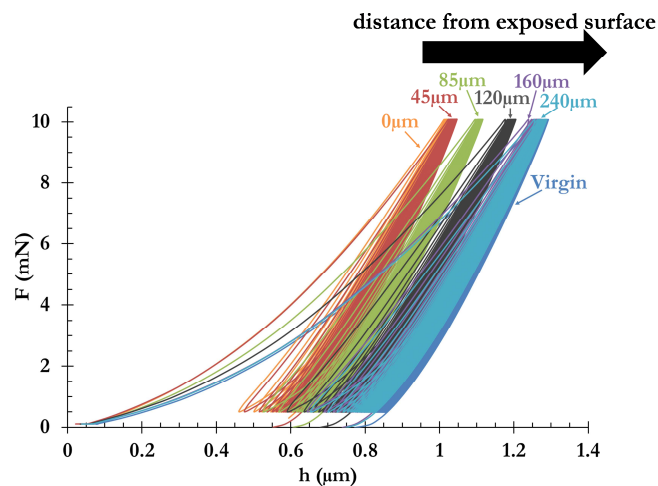


Figure 6. Load-displacement curves obtained at different distances from the exposed surface of a resin sample aged for 1005 h

From Figure 6, it can be observed that the curve measured at 240µm from the exposed surface is very close to that obtained on the surface of the virgin sample. As the distance from the external surface decreases, the curves are shifted to lower displacement values. The effect of decreasing distance from the surface on load displacement curves for the same aging time, is similar to that observed for the same distance and increasing aging time from Figure 5 and is typical of thermal oxidation of epoxy resins. The load-displacement curve obtained at the lowest distance on the cross section (45µm) is very close to that obtained on the external surface (0µm).

### **3.2 Change of mechanical properties with ageing on the exposed surface**

The surface indentation response presented in Figure 5 is analysed through the two parameters highlighted above: indentation reload modulus ( $E_{rel}^*$ ) and energy ratio ( $\eta$ ). Figures 7a and 7b show the evolution of both parameters with cycles for virgin and aged samples. The error bars (too small to be visible on most of the points) represent one standard deviation of 6 tests. The measurements performed on virgin and aged for 1005h composite samples are represented as well (empty markers). On both plots of  $E_{rel}^*$  and  $\eta$  evolution with cycles, one can distinguish an initial “transient stage”, in which they change rapidly (in less than 10 cycles), followed by a “steady state” in which the rate of change is lower and almost constant. However, this “steady state” is not a stabilised one since the response continues to change until the last cycle.

The reload modulus increases with cycles and with ageing time. The trend is similar between virgin and aged samples. As expected from the cyclic load-displacement curves, the properties measured on resin and composite are very close. However, the reload modulus measured on the composite is slightly higher than that measured on the resin, for both virgin and aged material.

The analysis of energy ratio presented in Figure 7b shows that its value for different aging times is significantly different only at the first cycle. In particular, the first cycle shows around 20% of drop of this parameter from the virgin to aged state. For the second and all further cycles, the difference between virgin and aged state is within the error bars. According to our analysis, it can be concluded that the amount of energy dissipated in viscoelastic strain, with respect to the total energy, is not affected by thermal ageing. The difference at first cycle highlights that the amount of plastic dissipation decreases with aging time. The decrease in energy dissipated to produce plastic strain is consistent with the “antiplasticization” phenomena observed by other authors from DMA spectra of aged samples [23-25]. In particular, it was shown that the beta transition peak progressively decreases with thermal ageing which induces a lower local chain mobility responsible for plastic strain. That is the reason why the material becomes more brittle, and thus less prone to undergo plastic strain, with thermal aging as observed by other authors [26-28]. Further investigations could provide a correlation between the energy ratio measured by instrumented indentation and beta dissipation measured by mechanical spectrometry. A slight difference in energy dissipation is observed between the resin and composite at the first cycle for both virgin and aged samples, while from the second cycle all the evolutions are superposed.



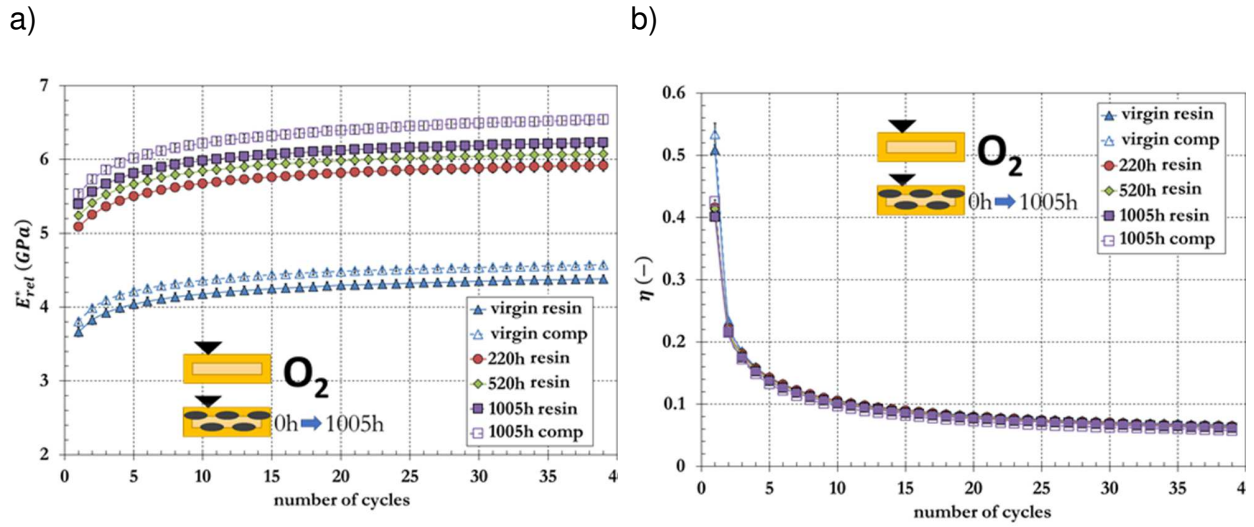


Figure 7. Evolution with cycles of reload modulus  $E_{rel}^*$  (a) and energy ratio  $\eta$  (b) on the external surface of virgin and aged resin and composite samples.

The richness of cyclic indentation tests could be useful to calibrate by reverse analysis a constitutive visco-elasto-plastic local behaviour law of virgin and oxidized polymers, avoiding the problem of non-uniqueness of solution occurring with a simple load-unload indentation test [29].

The values of cyclic indentation parameters at the first and at the last cycle (40<sup>th</sup>) measured on the external surface of both resin and composite at different aging times are presented in Table 1.

Aging time, h		$E_{rel,1}^*, GPa$	$E_{rel,40}^*, GPa$	$\eta_1, -$	$\eta_{40}, -$
0	resin	3.66±0.06	4.38±0.06	0.509±0.002	0.066±0.001
	composite	3.81±0.03	4.57±0.03	0.534±0.017	0.065±0.001
220	resin	5.09±0.05	5.92±0.08	0.416±0.002	0.064±0.001
	composite	5.14±0.06	6.05±0.07	0.431±0.003	0.061±0.001
520	resin	5.24±0.05	6.07±0.08	0.414±0.003	0.063±0.001

	composite	$5.45 \pm 0.06$	$6.42 \pm 0.11$	$0.416 \pm 0.002$	$0.061 \pm 0.001$
1005	resin	$5.39 \pm 0.06$	$6.23 \pm 0.06$	$0.401 \pm 0.001$	$0.061 \pm 0.01$
	composite	$5.53 \pm 0.06$	$6.54 \pm 0.07$	$0.425 \pm 0.003$	$0.057 \pm 0.001$

Table 1. Evolution of the indentation parameters at the first and last cycle with aging time of PR520 epoxy resin and composite surface

### 3.3. Gradients of mechanical properties in PR520 epoxy resin and composite

Thanks to the experimental procedure described in Figure 2, it was possible to evaluate the local properties change in the oxidized layer and to plot the property gradients as a function of the distance from the external surface for different aging conditions.

Figure 8 presents the reload indentation modulus (a) and the energy ratio (b) evaluated from indentation curves of Figure 6 (sample aged for 1005h) and plotted against the position of indentation print with respect to the exposed surface. For a better readability of the graph, only few cycles are reported: 1<sup>st</sup>, 2<sup>nd</sup>, 5<sup>th</sup>, 10<sup>th</sup>, 20<sup>th</sup> and last.

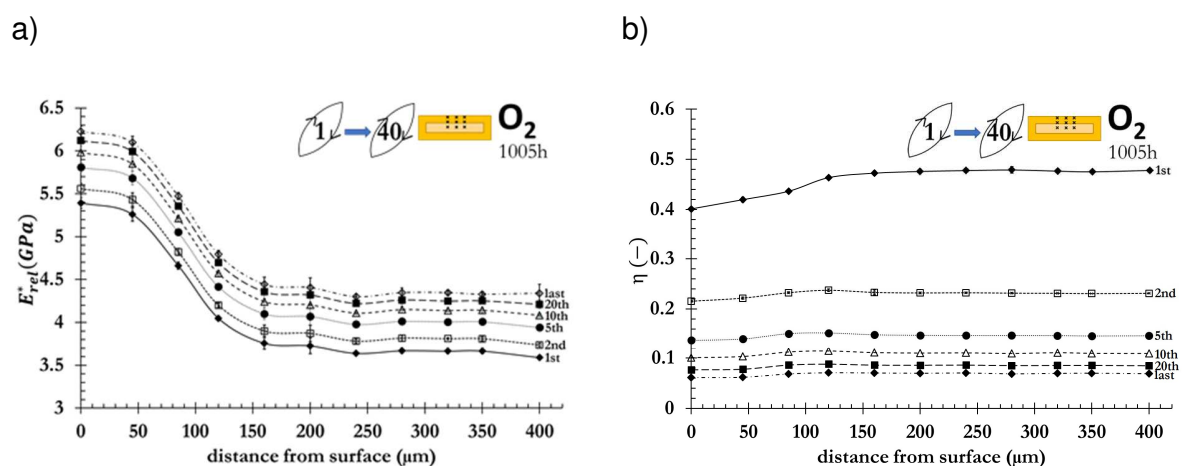


Figure 8. Evolution of reload modulus  $E_{rel}^*$  (a) and energy ratio  $\eta$  (b) of several indentation cycles as a function of the distance from the exposed surface for the neat resin sample aged for 1005h.

The shape of reload indentation modulus gradient profiles of different cycles (Figure 8a) are similar to each other and appear vertically shifted to higher modulus values as the cycle number increases. The reload indentation modulus progressively decreases to a plateau value from the surface to the sample core. The energy ratio profiles (Figure 8b) show a gradient through the oxidised layer only for the first cycle, while it is constant through the thickness from the second cycle. Unlike reload modulus, the energy ratio at the first cycle increases from the surface to the core, ending up stabilising to a constant value as well. According to our analysis, this suggests that the plastic behaviour is affected in the oxidised layer up to 120  $\mu\text{m}$ , while the viscoelastic behaviour is similar through the thickness.

Considering the similarities between gradients at second and further cycles, for better readability, only the first cycle is presented in Figure 9 for the resin and composite samples at other aging times. For the sake of comparison, the virgin samples were also tested following the same procedure at similar distances from the edge and presented in this figure. The gradient of elastic modulus in Figure 9a is qualitatively similar to the one obtained on different epoxy resins and for different aging conditions by other authors [3-8], despite the fact that the indentation modulus was determined from unloading in these references. The modulus of the virgin material is virtually constant through the sample thickness, while that of the aged samples is higher at the surface and it progressively decreases in the oxidized layer approaching the value measured on the virgin sample.

The value measured on the surface of aged samples is about 40% to 50% higher than that of the virgin material, depending on the aging time. Then, it decreases, quickly for the less severe aging condition and slowly for the higher aging time. Moreover, the profiles of the samples aged 520 *h* and 1005 *h* are virtually superposed from a distance from the external surface of about 70  $\mu\text{m}$ . The energy ratio  $\eta$  of the aged samples, presented in Figure 9b, is about 15-20% lower at the surface than that measured on the virgin sample. Then, it increases progressively through the thickness approaching the value of the virgin material. Moreover, it can be noted that, similarly to what observed on the profiles of reload modulus, the energy ratio measured through the oxidized layer of the less aged sample increases more quickly, while the profiles for the samples aged 520 *h* and 1005 *h* are quite close from a distance from the surface of 70  $\mu\text{m}$ .

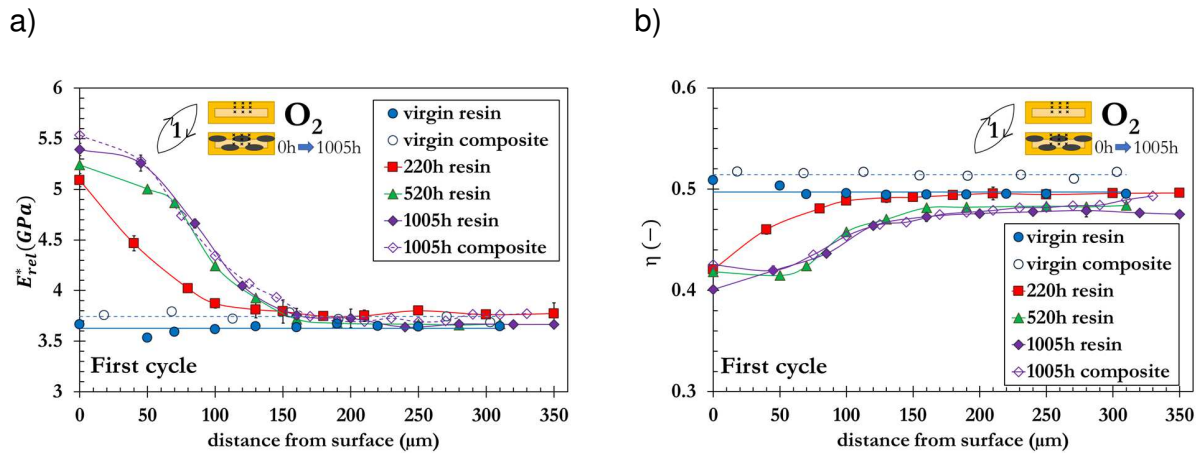


Figure 9. Evolution of reload modulus  $E_{rel}^*$  (a) and energy ratio  $\eta$  (b) at the first cycle as a function of the distance from the exposed surface of virgin and aged resin and composites samples.

A good agreement between the property gradient profiles measured in the oxidized layer of PR520 epoxy resin and composite can also be observed in Figure 9. In particular, both resin and composite reload moduli of the aged material decrease as the distance from the exposed surface increases, and stabilise to a value close to that of the virgin neat material at the same distance from the exposed surface. Similarly, the energy ratio of the first cycle increases with the distance from the sample edge for both resin and composite aged material and stabilizes to a value close, but slightly lower, than that measured on the virgin samples for the same distance from the exposed surface. However, a gap between resin and composite values is observed for the test performed on the surface directly exposed to the environment. To quantify this gap, the percent difference between resin and composite reload modulus and energy ratio of the first cycle measured at the same distance from the exposed surface of aged samples are reported in Table 2. The gap between virgin resin and composite material is reported as well in the first column considering the mean  $E_{rel}^*$  and  $\eta$  values along the thickness.

Distance from the surface	Virgin	Aged 1005h				
	Average along the thickness	0µm	45µm	120µm	200µm	280µm
$\left  \frac{E_{rel,1}^{*res} - E_{rel,1}^{*comp}}{E_{rel,1}^{*comp}} \right  \cdot 100$	3.0%	2.5%	0.4%	0.5%	0.7%	0.8%
$\left  \frac{\eta_1^{res} - \eta_1^{comp}}{\eta_1^{comp}} \right  \cdot 100$	3.4%	5.7%	<0.1%	0.3%	0.2%	1%

Table 2. Percent difference between reload modulus  $E_{rel}^*$  and energy ratio  $\eta$  of resin and composite for different distances from the edge of samples aged for 1005 h and through the thickness of virgin samples.

Table 2 confirms that the percent difference between neat and in-situ reload modulus measured on the surface of aged samples (about 2.5%) is similar to the difference evaluated between virgin samples (about 3%). However, the difference on energy ratio of aged samples is higher (about 6%) than that measured between virgin samples. It is interesting to observe that in the oxidized layer, for distances of 45, 120, 200 and 280 $\mu$ m from the exposed surface, the difference between resin and composite values is less than 1%. The comparison between the PR520 resin and its composite in virgin state on the surface and in the core was already reported in [21], attributing the slight difference measured on the surface to the curing degree related to thermal conditions during manufacturing.

Some authors [4] showed that the evolution of indentation modulus was proportional to the diffusion of oxygen and oxidation reaction. Therefore, although the values of mechanical properties are rather close at the surface of aged resin for different time, the shape of gradients in Figure 9a and b witnesses a significant difference in the mechanism of oxygen propagation between 220h and higher aging durations. At the first stages of aging, the oxygen diffuses through the thickness with low concentration producing oxidation reaction through the thickness up to *ca* 150  $\mu$ m. However, the oxidation reaction, which started throughout the layer, continues to progress slowly and embrittle the material. The absence of difference in mechanical properties for the thicknesses higher than 70-80  $\mu$ m after 520 h of aging shows that the oxygen diffusion was stopped at this distance between 220 and 520 h of aging time. After 1005h, only mechanical properties very close to surface might continue to change.

The profiles of mechanical property gradients allow moreover to estimate the thickness of the oxidized layer. It was assumed that the oxidation propagates as far as the difference between the measured reload modulus and that of the virgin sample is lower than 4%. The results are presented in Table 3, in which the thicknesses of oxidised layer estimated from indentation elastic moduli gradients on the same material aged at 120°C for similar aging times [27] are also reported. One can see that the thicknesses of the oxidized layer after aging at 150°C are significantly lower than those at 120°C for both aging times. Moreover, the authors [27] found a significantly lower increase of unload indentation modulus with respect to that of the virgin material: for the lowest distance from the exposed surface, the difference was 6.4% for the sample aged for 500 *h* and 9.8% for the sample aged for 1000 *h*. For similar ageing times, the difference between reload indentation of aged and virgin sample measured at the surface is of 43% and 47% respectively. In other words, for almost the same aging duration, oxygen penetrated more deeply in the case of aging at 120°C, but it has induced a significantly lower change in indentation modulus than at 150°C. The change of diffusion/reaction mechanism between 120°C and 150°C of aging might be attributed to the aging temperature close to the glass transition of the material.

thicknesses of the oxidized layer			increase in indentation modulus at the surface	
	120°C [27]	150°C	120°C [27] (unload modulus)	150°C (reload modulus)
~500 h	350±20µm	150±20µm	6.4%	43%

~1000 h	450±20µm	160±20µm	9.8%	47%
---------	----------	----------	------	-----

Table 3. Thickness of the oxidized layer, estimated from the indentation modulus gradient, of the PR520 resin aged in air for about 500 h and 1000 h at 150°C and 120°C [27]

## 4. Conclusions

In this work, the effects of thermal aging in air at 150°C on elastic, plastic and viscoelastic local properties of PR520 epoxy resin and composite have been studied through cyclic indentation tests. It has been shown that the kinetics of evolution of the reload indentation modulus ( $E_{rel}^*$ ) and the energy ratio ( $\eta$ ) with cycles is similar for virgin and thermally aged samples and that the amount of energy dissipated to produce time-dependent strain (the energy ratio from the second cycle) is not affected by thermal aging. Measurements performed along the thickness of aged samples, highlighted that the effect of decreasing distance from the surface on indentation loops for the same aging time, is similar to that observed for the same distance and increasing aging time. Reload modulus at all cycles and energy ratio at first cycle evolve in the oxidized layer approaching the value measured on the virgin sample, while the energy ratio from the second cycle is constant through the sample thickness and close to the value measured on the virgin sample. Property gradients due to thermal aging at 150°C for 1005 h, measured on the oxidized layer of PR520 epoxy resin and composite are virtually superposed showing that the thickness of the oxidized layer is quite similar for both materials. The difference between the two profiles for the same distance from the exposed surface is < 1%. Further investigations could improve this study to conclude



about the effect of thermal ageing on properties of matrix near fibers, in the so called “interphase”. It is maybe in this zone that a more significant difference in local properties exists. However, a lower indentation scale (nano) should be foreseen for such characterization to avoid any constraint effect of fiber bundles and thus measure the actual mechanical properties of the matrix.

## Acknowledgments

This work pertains to the domain of research of the French Government program “Investissements d’Avenir” (LABEX INTERACTIFS, reference ANR-11-LABX-0017-01; EQUIPEX GAP, reference ANR-11-EQPX-0018, EUR INTREE, reference ANR-18-EURE-0010). The authors thank the Poitou-Charentes Region for funding the PhD scholarship of Marina Pecora and SAFRAN-SNECMA (now SAFRAN Aircraft Engines) for providing the composite material. Pprime Institute gratefully acknowledges “Contrat de Plan Etat - Région Nouvelle-Aquitaine” (CPER) as well as the “Fonds Européen de Développement Régional (FEDER)” for their financial support to the reported work.

## References

- [1] J.P Pascault, H. Sautereau, J. Verdu, and R.J.J. Williams. Thermosetting Polymers. Marcel Dekker, Inc, 2002.
- [2] G.P. Tandon, E.R. Ripberger, and G.A. Schoeppner. Accelerated aging of pmr-15 resin at elevated pressure and/or temperature. *Proceedings of the SAMPE 2005 Symposium and Exhibition*, 2005.
- [3] L.L. Johnson, R.K. Eby, and M.A.B. Meador. Investigation of oxidation profile in pmr-15 polyimide using atomic force microscope (afm). *Polymer*, 44:187–197, 2003.

- [4] L. Olivier, N. Ho, J.C. Grandidier, and M.C. Lafarie-Frenot. Characterization by ultra-micro indentation of an oxidized epoxy polymer: Correlation with the predictions of a kinetic model of oxidation. *Polymer Degradation and Stability*, 93:489–497, 2008.
- [5] K.T. Gillen, R.L. Clough, and C.A. Quintana. Modulus profiling of polymers. *Polymer Degradation and Stability*, 17:31–47, 1987.
- [6] J. Wise, K.T. Gillen, and R.L. Clough. Quantitative model for the time development of diffusion-limited oxidation profiles. *Polymer*, 38:1929–1944, 1997.
- [7] M. Jiang, Y. Liu, C. Cheng, J. Zhou, B. Liu, M. Yu, and H. Zhang. Enhanced mechanical and thermal properties of monocomponent high performance epoxy resin by blending with hydroxyl terminated polyethersulfone. *Polymer Testing*, 69:302–309, 2018.
- [8] M. Minervino, M. Gigliotti, M.C. Lafarie-Frenot, and J.C. Grandidier. The effect of thermo-oxidation on the mechanical behaviour of polymer epoxy materials. *Polymer Testing*, 32(6):1020–1028, 2013.
- [9] K.V. Pochiraju and G.P. Tandon. Modeling thermo-oxidative layer growth in high temperature resins. *Journal of Engineering materials and Technology*, 128:107–116, 2006.
- [10] W.C. Oliver and G.M. Pharr. An improved technique for determining hardness and elastic modulus using load and displacement sensing indentation experiments. *Journal of Materials Research*, 7(6):1564–1583, 1992.
- [11] M. Hardiman, T.J. Vaughan, and C.T. McCarthy. The effects of pile-up, viscoelasticity and hydrostatic stress on polymer matrix nanoindentation. *Polymer Testing*, 52:157–166, 2016.
- [12] M.R. VanLandingham, J.S. Villarrubia, W.F. Guthrie, and G.F. Meyers. Nanoindentation of polymers: an overview. *Macromol. Symp.*, 167:15–43, 2001.

- [13] B J. Briscoe, L Fiori, and E W. Pelillo. Nano-indentation of polymeric surfaces. 31:2395–2405, 10 1998.
- [14] D. Tranchida, S. Piccarolo, J. Loos, and A. Alexeev. Mechanical characterization of polymers on a nanometer scale through nanoindentation. a study on pile-up and viscoelasticity. *Macromolecules*, 40:1259–1267, 2007.
- [15] T. Jin, X. Niu, G. Xiao, Z. Wang, Z. Zhou, G. Yuan, and al. Effects of experimental variables on pmma nano-indentation measurements. *Polymer Testing*, 41:1–6, 2015.
- [16] P.E. Mazeran, M. Beyaoui, M. Bigerelle, and M. Guigon. Determination of mechanical properties by nanoindentation in the case of viscous materials. *International Journal of Materials Research*, 103(6):715–722, 2012.
- [17] O. Smerdova, M. Pecora and M. Gigliotti. Cyclic indentation of polymers: Instantaneous elastic modulus from reloading, energy analysis, and cyclic creep. *Journal of Materials Research*, 34(21):3688-3698, 2019.
- [18] I.N. Sneddon: The relation between load and penetration in the axisymmetric boussinesq problem for a punch of arbitrary profile. *International Journal of Engineering Science*. 3, 47 (1965).
- [19] J.R. Gregory and S.M. Spearing. Nanoindentation of neat and in situ polymers in polymer-matrix composites. *Composites Science and Technology*, 65:595–607, 2005.
- [20] M. Hardiman, T.J. Vaughan, and C.T. McCarthy. The effect of fibre constraint in the nanoindentation of fibrous composite microstructures: A finite element investigation. *Computational Material Science*, 64:162–167, 2012.
- [21] M. Pecora, O. Smerdova and M. Gigliotti. In-situ characterization of the local mechanical behaviour of polymer matrix in 3D carbon fiber composites by cyclic indentation test. *Composite Structures*, 224:1-7, 2020.

- [22] M. Nowicki, A. Richter, B. Wolf and H. Kaczmarek. Nanoscale mechanical properties of polymers irradiated by UV. *Polymer*, 44: 6599:6606, 2003.
- [23] N. Rasoldier, X. Colin, J. Verdu, M. Bocquet, L. Olivier, et al. Model systems for thermo-oxidised epoxy composite matrices. *Composites: Part A*. 39:1522-1529, 2008.
- [24] M.C. Lafarie-Frenot., J. Grandidier, M. Gigliotti, L. Olivier, X. Colin, J. Verdu, J. Cinquin. Thermo-oxidation behaviour of composite materials at high temperatures: A review of research activities carried out within the COMEDI program. *Polymer Degradation and Stability*. 95(6):965-974, 2010.
- [25] J. Cinquin, X. Colin, B. Fayolle, M. Mille, S. Terekhina, et al. Thermo-oxidation behaviour of organic matrix composite materials at high temperatures. *Advances in Aircraft and Spacecraft Science*, Techno-Press, 3 (2):171-195, 2016.
- [26] K. Pochiaraju, G. Tandon, and G. Schoeppner. Evolution of stress and deformations in high-temperature polymer matrix composites during thermo-oxidative aging. *Mechanics of Time-Dependent Materials*, 12(45-68), 2008.
- [27] M. Pecora, Y. Pannier, M.C. Lafarie-Frenot, M. Gigliotti, and C. Guigon. Effect of thermo-oxidation on the failure properties of an epoxy resin. *Polymer Testing*, 52:209–217, 2016.
- [28] E. Ernault, E. Richaud, and B. Fayolle. Origin of epoxies embrittlement during oxidative aging. *Polymer Testing*, 63:448–454, 2017.
- [29] M. C. Barick, Y. Gaillard, A. Lejeune, F. Amiot, F. Richard. On the uniqueness of intrinsic viscoelastic properties of materials extracted from nanoindentation using FEMU. *International Journal of Solids and Structures*, 202:929:946, 2020.

# Graphical Abstract

